

Quenched lattice QCD at finite isospin density and related theories.

J. B. Kogut

*Dept. of Physics, University of Illinois,
1110 West Green Street, Urbana, IL 61801-3080, USA*

D. K. Sinclair

*HEP Division, Argonne National Laboratory,
9700 South Cass Avenue, Argonne, IL 60439, USA*

Abstract

We study quenched QCD at finite chemical potential, μ_I , for the third component of isospin and quenched two-colour QCD at finite chemical potential, μ , for quark number. In contrast to the quenched approximation to QCD at finite quark-number chemical potential, the quenched approximations to these theories behave similarly to the full theories. The reason is that these theories have real positive fermion determinants. In both of these theories there is some critical chemical potential above which the charge coupled to the chemical potential is spontaneously broken. In each case, the transition appears to be second order. We study the scaling properties near the critical point using scaling functions suggested by effective (chiral) Lagrangians and find evidence for scaling with mean-field critical exponents in each case. The subtleties associated with observing the critical scaling of these theories are discussed.

I. INTRODUCTION

RHIC at Brookhaven and the CERN heavy-ion program give us the possibility of producing hadronic matter at high temperatures and finite baryon number density. Cold nuclear matter – hadronic matter at finite baryon number density – exists in neutron stars. In addition, the bulk properties of large nuclei should be well described as nuclear matter. Because of Coulomb interactions, nuclear matter is not only at finite baryon-number density but also finite (negative) isospin(I_3) density. Finally, it has been suggested that sufficiently dense nuclear matter will also have finite strangeness density. It is therefore of interest to study QCD at finite baryon-number, isospin and strangeness densities both at zero and finite temperature.

Such finite densities are achieved by introducing a chemical potential for the relevant charge operator. Unfortunately, the introduction of a finite chemical potential for quark/baryon number leads to a complex fermion determinant which precludes the use of standard simulation methods based on importance sampling. Introducing a chemical potential μ_I for the third component (I_3) of isospin leaves the determinant real and non-negative. Adding the additional (small) I_3 breaking term needed to observe spontaneous isospin breaking on a finite (lattice) volume, makes this determinant strictly positive and simulations possible. Effective Lagrangian analyses of this theory have indicated that it should undergo a phase transition at $\mu_I = m_\pi$ to a state where I_3 is spontaneously broken by a charged pion condensate with an accompanying Goldstone mode [1] We are currently performing simulations of this theory [2, 3]. Adding, in addition, a finite chemical potential (μ_s) for strangeness again makes the fermion determinant complex. In this case, however, there are related theories with real positive fermion determinants which mimic the correct physics for small μ_s [2].

Until we have a satisfactory way of dealing with finite baryon-number density, it is of interest to study models which exhibit some of the anticipated properties of QCD at finite quark/baryon-number density but which have real positive fermion determinants. One such model is 2-colour QCD at finite quark-number chemical potential (μ). This theory exhibits diquark condensation for μ sufficiently large. [4, 5, 6, 7, 8, 9] Effective Lagrangians and chiral perturbation theory analyses of this theory display similar behaviour, and give quantitative

predictions for the nature of this transition and the equation of state in the neighbourhood of this critical point [10, 11]. These predictions have been validated in the strong coupling limit of 2-colour QCD at finite μ by Aloisio et al. [8]. Formation of such condensates has been suggested for QCD at large enough μ [12, 13, 14, 15, 16]. There is, of course, one crucial difference. The condensate for 2-colour QCD is a colour singlet, the symmetry breaking is realized in the Goldstone mode and this theory exhibits superfluidity. For true, 3-colour QCD, the condensate is, of necessity, coloured, the symmetry breaking is realized in the Higgs mode and this theory exhibits colour superconductivity.

The quenched approximation, i.e. the approximation of setting the fermion determinant to unity has proved useful for calculating hadron spectra and matrix elements. At finite temperatures it shows the deconfinement transition at which chiral symmetry is restored, as does the full theory. However, since the order of this transition and the equation of state are flavour dependent, it yields no useful information on these issues. Where it can be used, its principal advantage is that it reduces the computing requirements by several orders of magnitude. For QCD at finite quark-number chemical potential, the quenched approximation was even more appealing, since it avoids the problem of the complex fermion determinant. Unfortunately, it was soon discovered that it does not produce the correct physics [17, 18, 19]. Whereas it is believed that as μ is increased, the first phase transition should occur for $\mu \sim m_N/3$, the quenched theory showed a transition for $\mu \approx m_\pi/2$. This was realized to indicate that the quenched theory should be considered as the zero-flavour limit of a theory with an equal number of quark flavours with quark-number +1 and with quark-number -1, rather than of a theory where all the quarks have quark number +1. This was implicit in this early work [17, 18, 19], and was made explicit in terms of random matrix models by Stephanov [20].

Since QCD at finite isospin chemical potential has equal numbers of quarks with $I_3 = +\frac{1}{2}$ and with $I_3 = -\frac{1}{2}$, it thus should be expected to admit a sensible quenched approximation. What one immediately realizes is that earlier studies of quenched QCD at finite quark-number chemical potential [17, 18, 19, 21] can now be reinterpreted as studies of quenched QCD at finite isospin chemical potential.

Now, however, we can include an explicit I_3 violating interaction which makes the Dirac operator positive definite (rather than positive semi-definite) giving better conver-

gence for our inversion algorithm, and allowing us to measure the I_3 -breaking pion condensate directly. Similarly, in 2-colour QCD, since quarks and antiquarks belong to the same representation (the fundamental) of $SU(2)_{colour}$, it too should have a sensible quenched approximation. In fact, we see, it is the same property that gives these theories real positive fermion determinants that allows quenched approximations. This is not surprising, since all a positive fermion determinant does is to reweight the contributions. This contrasts with a determinant where the sign of the real part changes and contributions from different configurations can (and in the case of QCD at finite μ must) cancel.

Once one has determined that each of these theories undergoes a second order transition to a state characterized by a condensate which spontaneously breaks the charge coupled to the chemical potential, it is useful to examine the scaling properties of the order parameter and certain composite operators in the vicinity of the critical point and to obtain the critical exponents. This allows one to write down an equation of state for the system. Such equations of state are important for modeling neutron stars. Of course there one needs to work at finite baryon-number chemical potential as well. Effective Lagrangians and chiral perturbation theory through 1-loop suggest that we should see mean field scaling near this critical point [1, 10, 11].

We have measured the pion condensates, chiral condensates and isospin densities as functions of isospin chemical potential (μ_I) and the explicit isospin breaking parameter λ on $12^3 \times 24$ and 16^4 quenched QCD gauge configurations at $\beta = 6/g^2 = 5.7$, and on 8^4 quenched gauge configurations at $\beta = 5.5$. Both show evidence for the expected mean-field scaling. In addition we have measured the diquark condensate, chiral condensate and quark-number density on a set of 8^4 and 12^4 quenched 2-colour QCD configurations with $\beta = 4/g^2 = 2.0$. Here mean-field scaling is again favored.

In section 2 we present our actions and their relevant symmetries. Section 3 describes our simulations and results. Critical scaling analyses are presented in section 4. Discussions and conclusions are presented in section 5.

II. ACTIONS AND SYMMETRIES

The staggered fermion part of the action for lattice QCD with degenerate u and d quarks at a finite chemical potential μ_I for isospin (I_3) is

$$S_f = \sum_{sites} [\bar{\chi}[\mathcal{D}(\tau_3\mu_I) + m]\chi + i\lambda\epsilon\bar{\chi}\tau_2\chi] \quad (1)$$

where $\mathcal{D}(\mu)$ is the standard staggered \mathcal{D} with links in the $+t$ direction multiplied by $e^{\frac{1}{2}\mu}$ and those in the $-t$ direction multiplied by $e^{-\frac{1}{2}\mu}$. The explicit symmetry breaking term $i\lambda\epsilon\chi^T\tau_2\chi$, the lattice equivalent of $i\lambda\bar{\psi}\gamma_5\tau_2\psi$, is in a direction in which the I_3 symmetry is expected to break spontaneously for μ_I sufficiently large. This term is necessary in order to observe spontaneous symmetry breaking from a finite lattice. We will be interested in the limit $\lambda \rightarrow 0$. We will present a detailed discussion of the symmetries of this theory in a forthcoming paper on our simulations with dynamical quarks. The Dirac operator

$$\mathcal{M} = \begin{bmatrix} \mathcal{D}(\mu_I) + m & \lambda\epsilon \\ -\lambda\epsilon & \mathcal{D}(-\mu_I) + m \end{bmatrix} \quad (2)$$

has determinant

$$\det \mathcal{M} = \det[\mathcal{A}^\dagger \mathcal{A} + \lambda^2] \quad (3)$$

where we have defined

$$\mathcal{A} \equiv \mathcal{D}(\mu_I) + m. \quad (4)$$

We note that this determinant is positive for $\lambda \neq 0$, as promised. Observables we measure include the chiral condensate

$$\langle \bar{\psi}\psi \rangle \Leftrightarrow \langle \bar{\chi}\chi \rangle, \quad (5)$$

the charged pion condensate

$$i\langle \bar{\psi}\gamma_5\tau_2\psi \rangle \Leftrightarrow i\langle \bar{\chi}\epsilon\tau_2\chi \rangle \quad (6)$$

and the isospin density

$$j_0^3 = \frac{1}{V} \left\langle \frac{\partial S_f}{\partial \mu_I} \right\rangle. \quad (7)$$

The quark action for 2-colour QCD with one staggered quark is

$$S_f = \sum_{sites} \left\{ \bar{\chi}[\mathcal{D}(\mu) + m]\chi + \frac{1}{2}\lambda[\chi^T\tau_2\chi + \bar{\chi}\tau_2\bar{\chi}^T] \right\} \quad (8)$$

where $\mathcal{D}(\mu)$ is the normal staggered covariant finite difference operator with μ introduced by multiplying the links in the $+t$ direction by e^μ and those in the $-t$ direction by $e^{-\mu}$. The superscript T stands for transposition. The term proportional to λ explicitly breaks quark-number symmetry, and again we shall be interested in the limit $\lambda \rightarrow 0$. The symmetries of this action and the positivity of the determinant and pfaffian have been discussed extensively in previous work on dynamical quark simulations and will not be repeated here [4, 5, 6, 7].

The observables we measure include the chiral condensate,

$$\langle \bar{\chi}\chi \rangle = \langle \bar{\psi}\psi \rangle, \quad (9)$$

the diquark condensate,

$$\langle \chi^T \tau_2 \chi \rangle \quad (10)$$

and the quark-number density

$$j_0 = \frac{1}{V} \left\langle \frac{\partial S_f}{\partial \mu} \right\rangle. \quad (11)$$

III. QUENCHED SIMULATIONS AT FINITE CHEMICAL POTENTIALS

A. Quenched QCD at finite isospin chemical potential

We have calculated quark propagators at a finite chemical potential μ_I for the third component, I_3 , of isospin from a noisy source on an ensemble of $12^3 \times 24$ and 16^4 quenched gauge field configurations at $\beta = 5.7$ and on 8^4 quenched gauge field configurations at $\beta = 5.5$. From these propagators we obtained stochastic estimators for the pion condensate, the chiral condensate and the isospin density as functions of μ_I and the I_3 breaking parameter λ . We chose $\lambda \ll m$, since we are interested in the limit $\lambda \rightarrow 0$.

Let us first consider the $\beta = 5.7$ calculations. We generated 100 $\beta = 5.7$ $12^3 \times 24$ equilibrated configurations separated by 1000 sweeps consisting of 9 overrelaxation sweeps followed by 1 10-hit metropolis sweep repeated 100 times, which appeared to generate relatively independent configurations. On each of these configurations we obtained a stochastic estimate of $i\langle \bar{\chi}\epsilon\tau_2\chi \rangle$, $\langle \bar{\chi}\chi \rangle$ and j_0^3 using a single noisy source, for $m = 0.025$, $\lambda = 0.0025, 0.005, 0.0075$ (and $\lambda = 0$ for $\mu_I < \mu_c$) and $\mu_I = 0.0, 0.1, 0.2, 0.3, 0.35, 0.4, 0.45, 0.5, 0.55, 0.6, 0.7, 0.8, 0.9, 1.0, 1.2, 1.6, 1.8, 2.0, 2.1$. The

fact that we used the same set of configurations and noise vectors for each value of λ and μ_I means that all our ‘data’ points are strongly correlated. We also measured the pion mass at $\mu = \lambda = 0$ using a wall source, on these configurations gauge fixed to Coulomb gauge. We obtained $m_\pi = 0.441(1)$. Runs at $\lambda = 0.0025$ were performed on an 8^4 lattice at selected μ_I values to check that finite size effects were not too large.

From these $12^3 \times 24$ measurements we determined that the neighbourhood of $\mu_I = 0.45$ was of particular interest. We then increased our spatial volume and performed simulations on a 16^4 lattice, again at $\beta = 5.7$ and $m = 0.025$, to allow us to run at smaller λ . Here we generated our quenched configurations and performed our measurements of the condensates and isospin density using the same hybrid molecular-dynamics code that we use for simulations with dynamical quarks. This meant that we used an independent set of configurations for each value of λ and μ_I . 100 independent configurations separated by 10 molecular-dynamics time units were generated for each λ and μ_I . (With no fermions in the updating, 10 time units were adequate to decorrelate configurations. The time increment for updating was $dt = 0.1$ which is adequate without light fermions in the updating.) We chose $\lambda = 0.000625, 0.00125, 0.001875, 0.0025$, and used $\mu_I = 0.2, 0.25, 0.3, 0.35, 0.375, 0.4, 0.425, 0.45, 0.475, 0.5, 0.525, 0.55, 0.6, 0.65, 0.7$ to adequately cover the region of interest.

The charged pion condensates are shown in figure 1. What is immediately clear is that the condensate is small for small μ_I . At $\mu_I = 0$, the condensate vanishes as $\lambda \rightarrow 0$. Aloisio *et al.*[8] have shown that this vanishing of the condensate extends to small but finite μ_I . We have performed various extrapolations to $\lambda = 0$ — linear, linear plus cubic, linear plus quadratic — all of which are based on the predictions of partially conserved current analyses and their implementations in effective (chiral) Lagrangian models. These extrapolations suggest that this condensate vanishes out to at least $\mu_I \approx 0.4$. (the $\lambda = 0$ measurements are trivially zero and do not enter into this discussion). More importantly, these extrapolation schemes, and those based on power law scaling in λ as would be expected for μ_I at a critical value, indicate that it is highly probable that this condensate remains finite as $\lambda \rightarrow 0$ in the infinite volume limit for $\mu_I \gtrsim 0.5$. This indicates that there is a phase transition for $\lambda = 0$ at some $\mu_I = \mu_c$ with $0.4 \lesssim \mu_I \lesssim 0.5$, below which the pion condensate is zero and above which there is a non-zero charged pion condensate which breaks I_3 spontaneously with associated

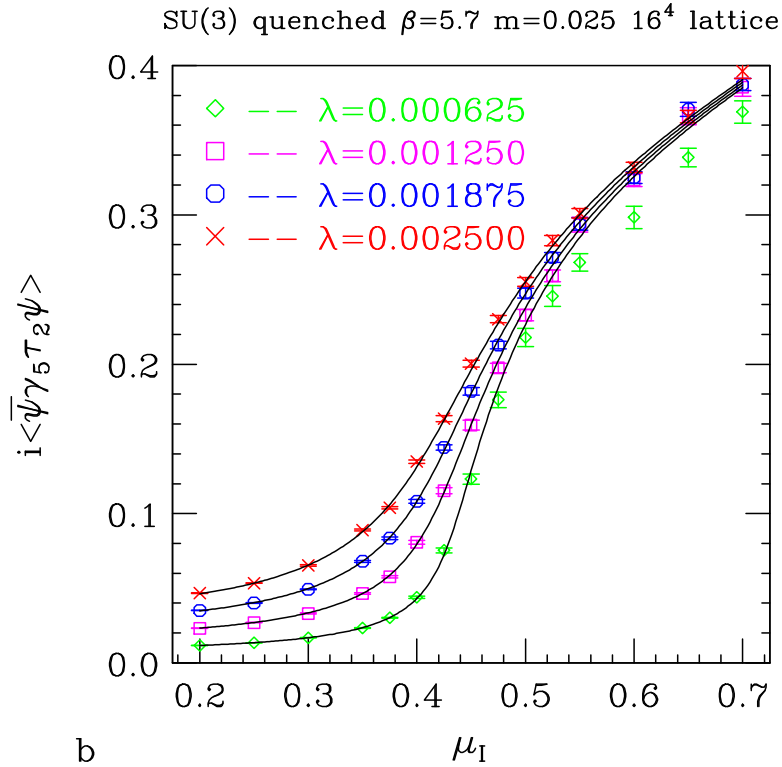
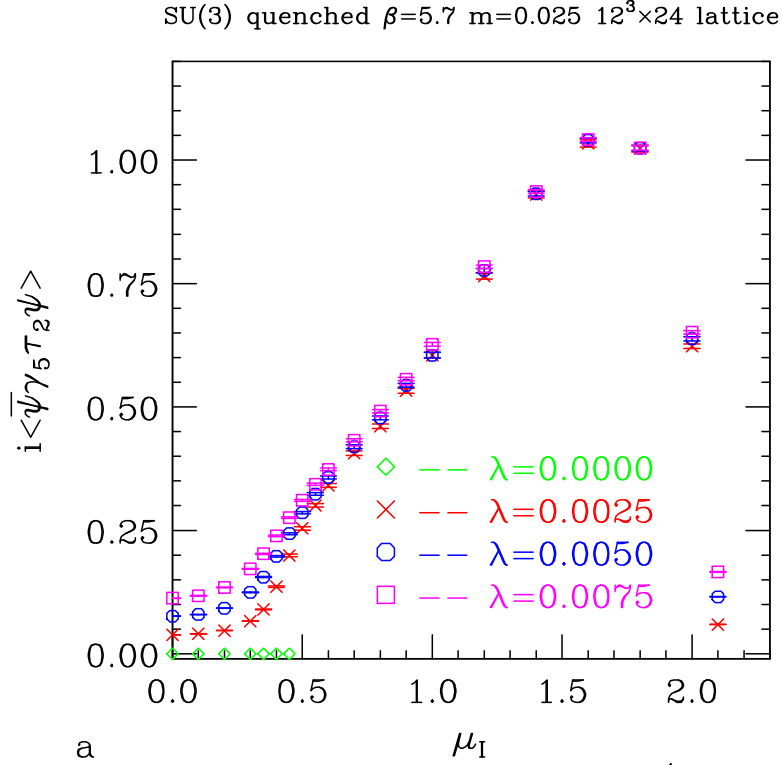


FIG. 1: a) Charged pion condensate, $i\langle\bar{\psi}\gamma_5\tau_2\psi\rangle = i\langle\bar{\chi}\epsilon\tau_2\chi\rangle$, as a function of μ_I , on a $12^3 \times 24$ lattice with $\beta = 5.7$ and quark mass $m = 0.025$. b) Charged pion condensate on a 16^4 lattice. The solid lines superimposed on our measurements are the scaling fits described in section 4.

Goldstone pions. Since there is no abrupt jump at $\mu_I = \mu_c$, this suggests that the phase transition is second order. This condensate increases monotonically up to $\mu_I \gtrsim 1.6$ after which it falls rather rapidly approaching zero by $\mu_I \approx 2.0$. This fall is clearly a saturation effect, a conclusion that becomes even more compelling when we look at j_0^3 .

SU(3) quenched $\beta=5.7$ $m=0.025$

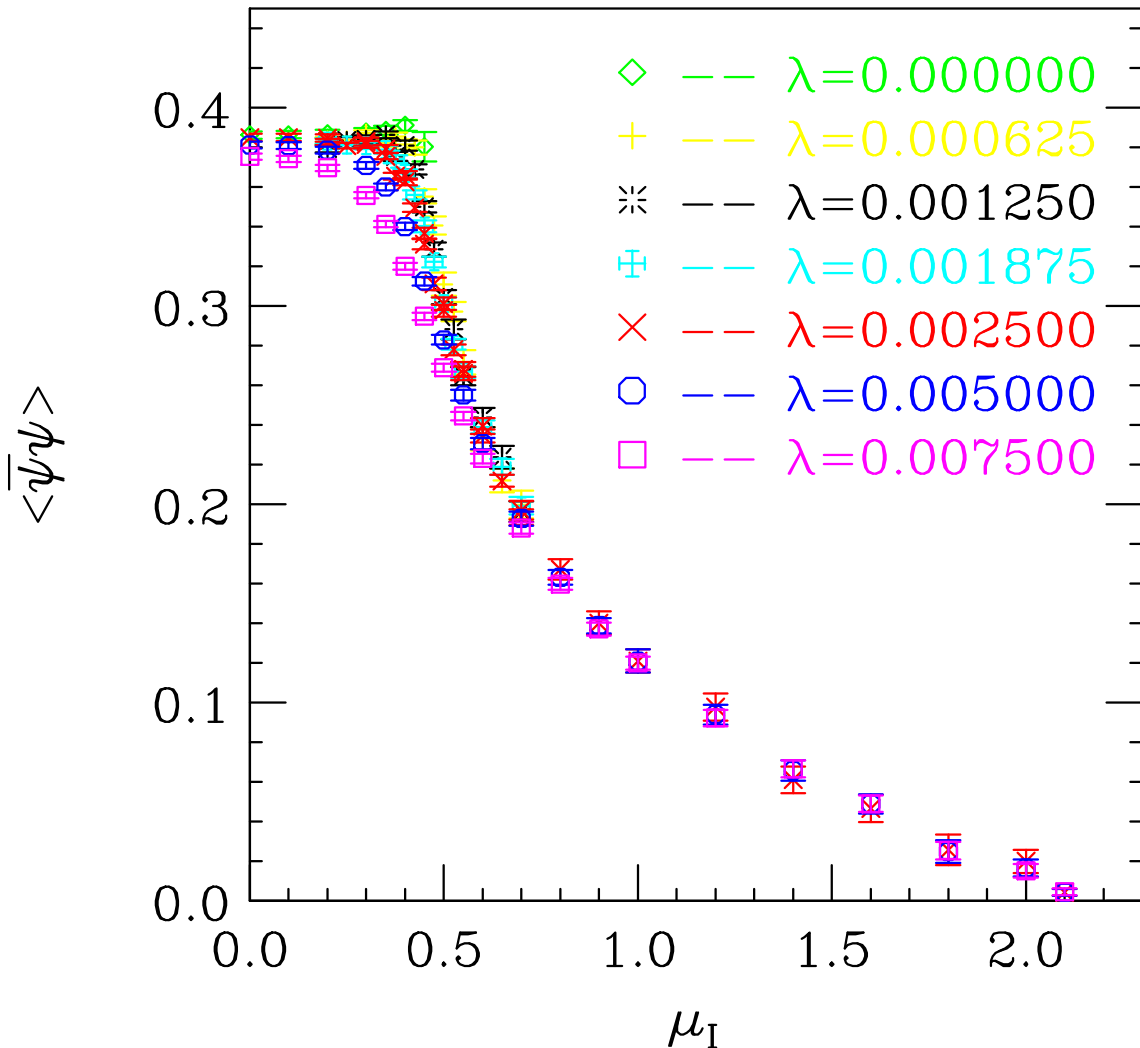


FIG. 2: The chiral condensate, $\langle \bar{\psi}\psi \rangle = \langle \bar{\chi}\chi \rangle$, at $\beta = 5.7$ and $m = 0.025$ as a function of μ_I .

Figure 2 shows the chiral condensate as a function of μ_I for both the $12^3 \times 24$ and 16^4 simulations at $\beta = 5.7$, $m = 0.025$. We see that it remains approximately constant at its $\mu = 0$ values for $\mu_I < \mu_c$, above which it commences its descent towards zero. What is also clear when looking at the plots of chiral and pion condensates, is that the expectation from tree level chiral perturbation theory that the condensate merely rotates from the chiral

symmetry breaking to the isospin breaking direction has at best a rather limited range of validity.

SU(3) quenched $\beta=5.7$ $m=0.025$

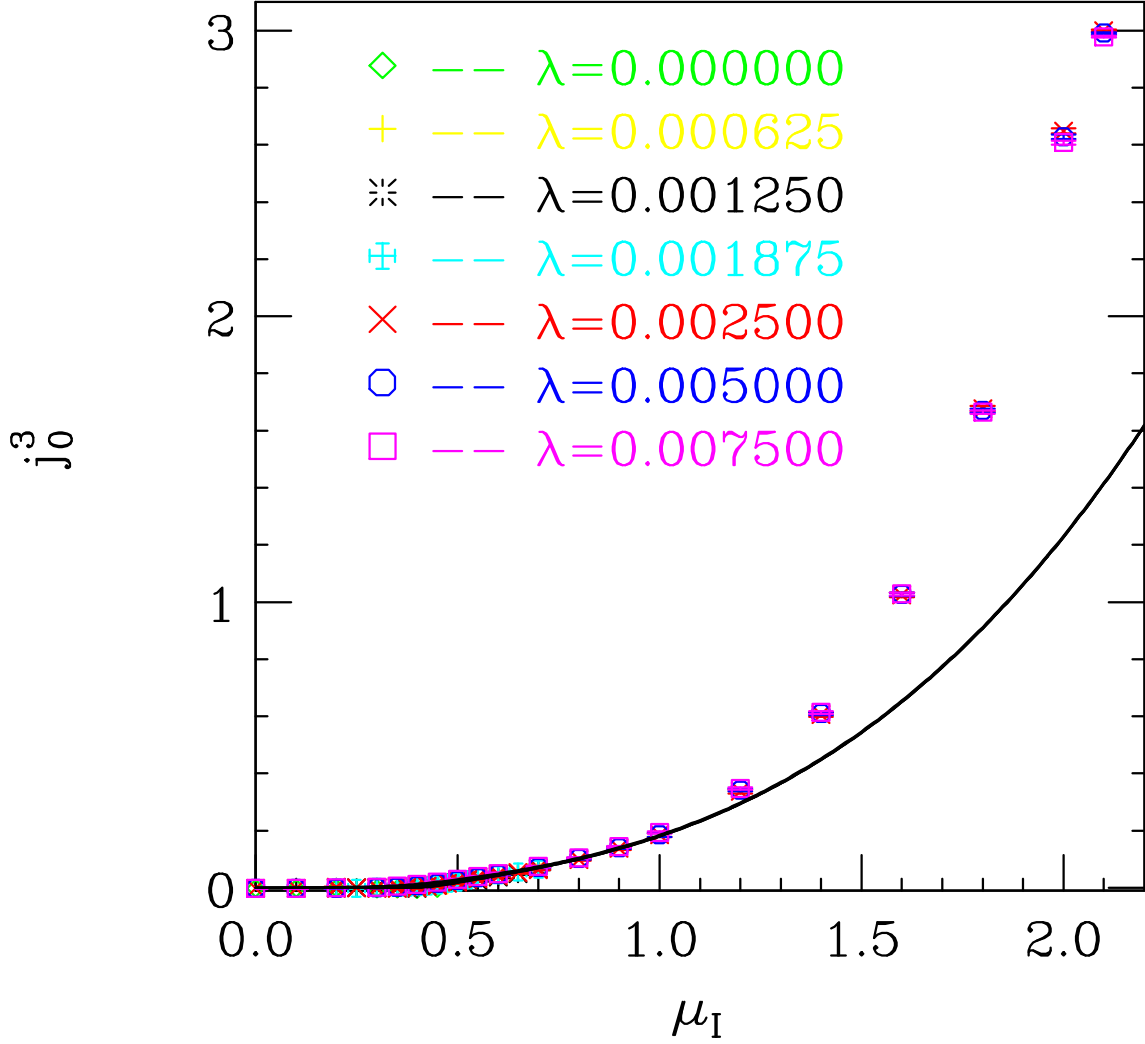


FIG. 3: Isospin density at $\beta = 5.7$ and $m = 0.025$ as a function of μ_I . The curves are from the scaling fits to the pion condensate, and are described in section 4

The isospin density is presented in figure 3. The main features are its slow rise from zero above μ_c , followed by a more rapid rise at larger μ_I , finally flattening out at its saturation value of 3 for $\mu_I \gtrsim 2.0$. Note that the saturation value is 3 because we have chosen to normalize it to 8 continuum flavours, the number associated with the action given in section 2. The value 3 arises from $\frac{1}{2}$ for each of 3 colours and 2 staggered ‘flavours’ (= 8 continuum flavours) on each site, the maximum allowed by fermi statistics. (For contrast

the condensates have been normalized to 4 flavours for comparison with those reported in finite temperature simulations.)

We now turn to the consideration of our simulations and measurements at stronger coupling, $\beta = 5.5$, which were performed on an 8^4 lattice. Again we chose $m = 0.025$ in lattice units. Here we followed the same procedure as for the $\beta = 5.7$, 16^4 simulations, using the same hybrid molecular-dynamics code as used for our dynamical simulations. We used $\lambda = 0.0025, 0.005, 0.0075$ (and $\lambda = 0$ for $\mu_I < \mu_c$) in lattice units. Our chosen μ_I (in lattice units) were $0.0, 0.1, 0.2, 0.3, 0.35, 0.4, 0.45, 0.5, 0.6, 0.7, 0.8, 0.9, 1.0, 1.2, 1.4, 1.6, 1.8, 2.0, 2.2$. We checked for finite size effects, by repeating these simulations on a 12^4 lattice for selected μ_I values ($0.3, 0.4, 0.5, 0.6, 0.8$ and 1.0), with $\lambda = 0.0025$ where such effects are expected to be largest, again analyzing 100 configurations for each μ_I . For each μ_I the difference between the 8^4 and 12^4 measurements was within 2 standard deviations of zero.

The I_3 -breaking charged pion condensate is plotted in figure 4 as a function of μ_I , for the λ values mentioned above. Superficially, this graph appears similar to figure 1. Again, we note that any reasonable extrapolation to $\lambda = 0$ would suggest that, in this limit, the condensate vanishes for $\mu_I \leq 0.3$, while it clearly does not for $\mu_I \geq 0.5$, which strongly suggests that there is a phase transition at $\mu_I = \mu_c$ with μ_c lying in the range 0.3 – 0.5 . (We have not performed such extrapolations since at larger μ_I values, statistical fluctuations lead to incorrect ordering of the condensates for different λ s, which would produce unphysical extrapolations.) However, what one notices on closer inspection is that the transition is somewhat steeper than that for $\beta = 5.7$. We will return to this point in the next section. Saturation again sets in for μ_I a little above 2.0 .

The chiral condensate shown in figure 5 behaves very similarly to that at $\beta = 5.7$. The main reason for presenting it here is to display the scaling predictions of section 4. We note, however, that its value is $0.764(7)$ at $\lambda = \mu_I = 0$, so again it is at most over a limited range of μ_I that the condensate simply rotates from the chiral towards the isospin-breaking direction. However, the violations are less severe than at $\beta = 5.7$. The isospin density also behaves very similarly to that at weaker couplings, rising steadily from zero as μ_I is increased past μ_c and eventually saturating at 3. This is plotted in figure 6 again, primarily to show the scaling predictions described in the next section.

SU(3) quenched $\beta=5.5$ $m=0.025$ 8^4 lattice

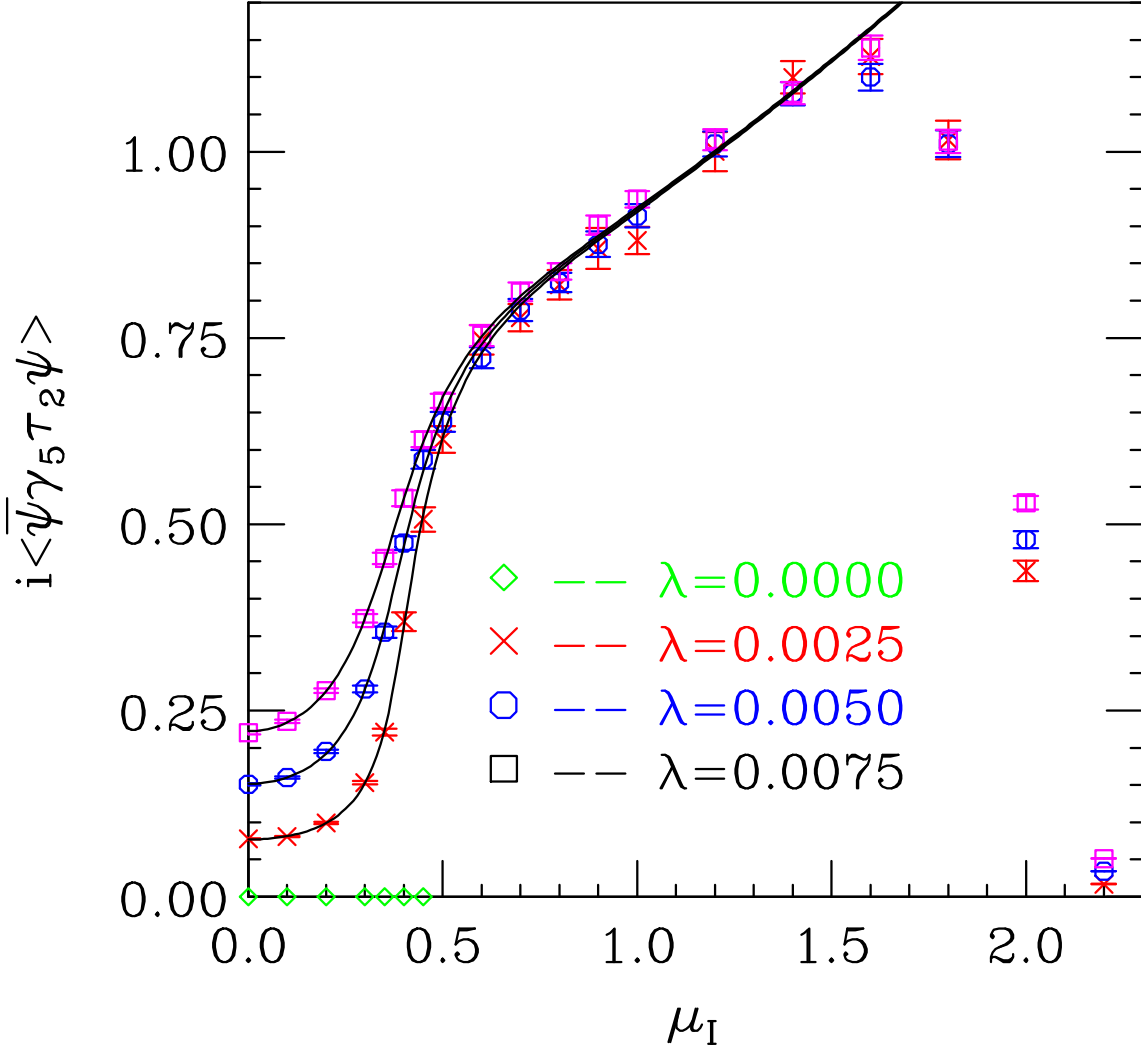


FIG. 4: Charged pion condensate as a function of μ_I and λ on an 8^4 lattice with $\beta = 5.5$ and $m = 0.025$. The solid lines are fits described in section 4.

B. 2-colour QCD at finite quark-number chemical potential.

We calculated the quark propagators for fundamental staggered quarks at finite chemical potential μ from a single noisy source for each of a set of quenched SU(2) gauge field configurations at $\beta = 2.0$. These configurations were generated using the hybrid molecular-dynamics code of our dynamical quark simulations. We generated 100 such independent gauge configurations spaced by 10 molecular-dynamics time units for each μ and λ value. Our simulations used $dt = 0.1$ for the up-

SU(3) quenched $\beta=5.5$ $m=0.025$ 8^4 lattice

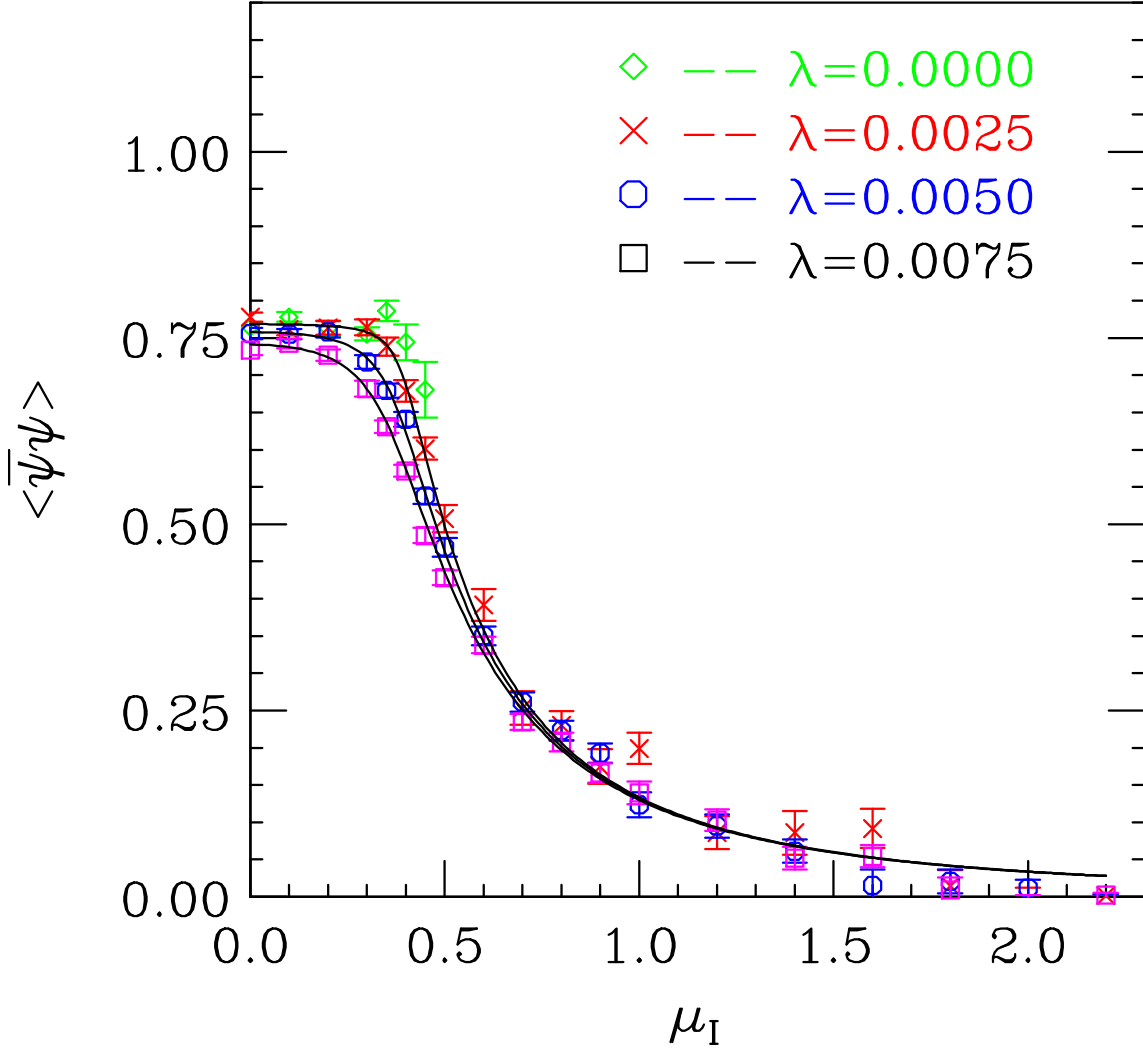


FIG. 5: The chiral condensate as a function of μ_I for quenched QCD at $\beta = 5.5$, $m = 0.025$. The solid lines are fits derived from the scaling analyses of section 4.

dating. We used $\lambda = 0.0025, 0.005, 0.0075, 0.01$ (and zero for $\mu < \mu_c$), for $\mu = 0.0, 0.1, 0.15, 0.175, 0.2, 0.21, 0.225, 0.25, 0.3, 0.4, 0.5, 0.6, 0.7, 0.8, 0.9, 0.95, 1.0, 1.1$, which adequately covered the range of interest. Since the 8^4 ‘data’ showed evidence of finite size effects, we repeated these simulations on a 12^4 lattice. From these noisy quark propagators we obtained stochastic estimators for the diquark condensate, the chiral condensate and the quark-number density, each normalized to 4 continuum flavours (1 staggered quark field).

Figure 7 shows the diquark condensate as a function of μ for each of the considered

SU(3) quenched $\beta=5.5$ $m=0.025$ 8^4 lattice

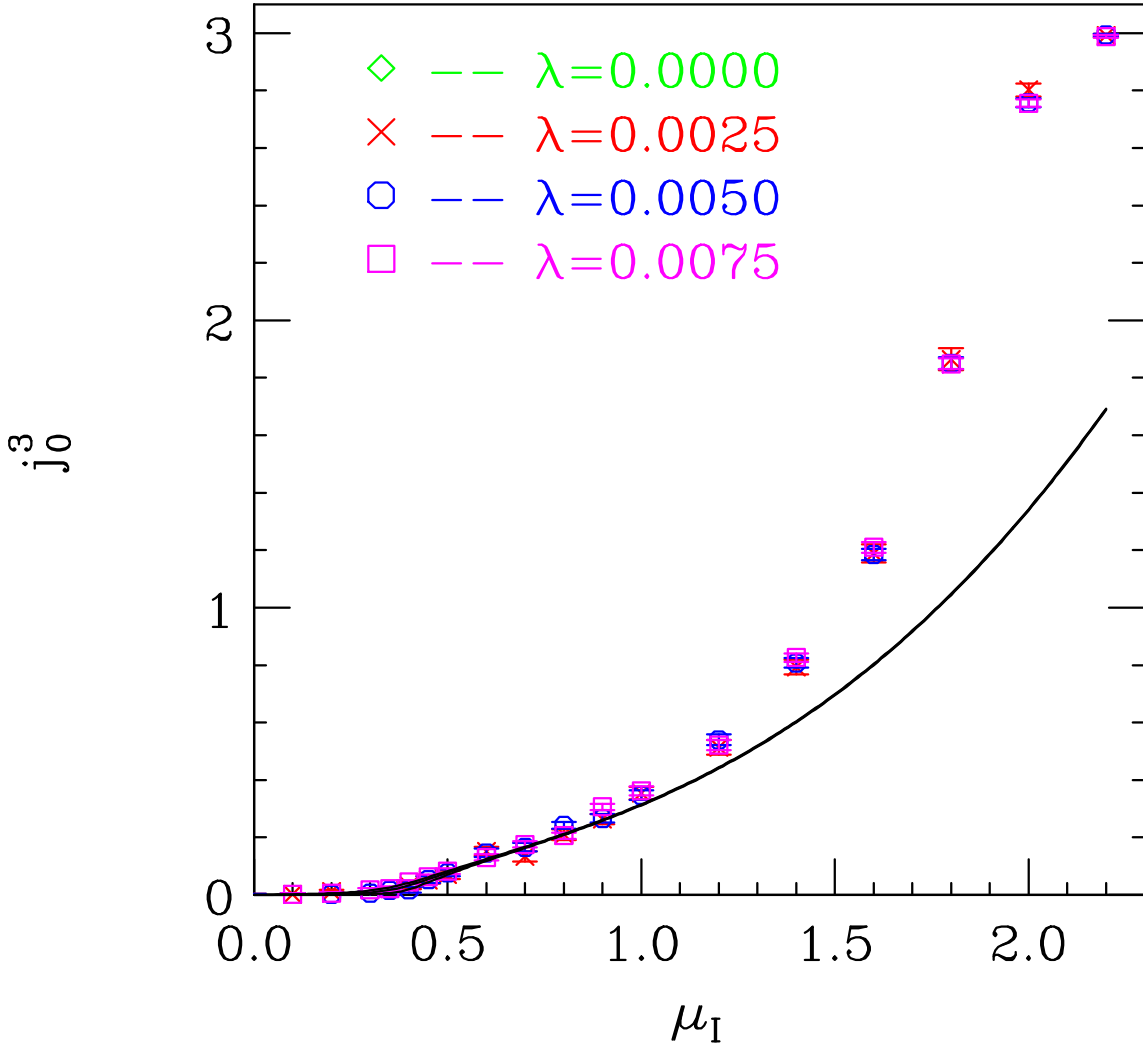


FIG. 6: The isospin density as a function of μ_I for quenched QCD at $\beta = 5.5$, $m = 0.025$. The solid lines are fits derived from the scaling analyses of section 4.

λ values. For $\mu \leq 0.15$ it is clear that any reasonable extrapolation to $\lambda = 0$ from finite λ would yield estimates close to zero for the condensate in this limit. For $\mu \geq 0.25$, the extrapolated condensate clearly remains greater than zero for $\lambda \rightarrow 0$. Thus we deduce that there is a phase transition at $\mu = \mu_c$ from the normal state to one in which quark number is broken spontaneously by a diquark condensate, for some μ_c between 0.15 and 0.25. Such a symmetry breaking would be accompanied by a diquark Goldstone boson. The reason we have not performed an extrapolation in λ is clear when one looks at the behaviour of the condensate at $\lambda = 0.0025$ relative to the higher lambdas. We note that

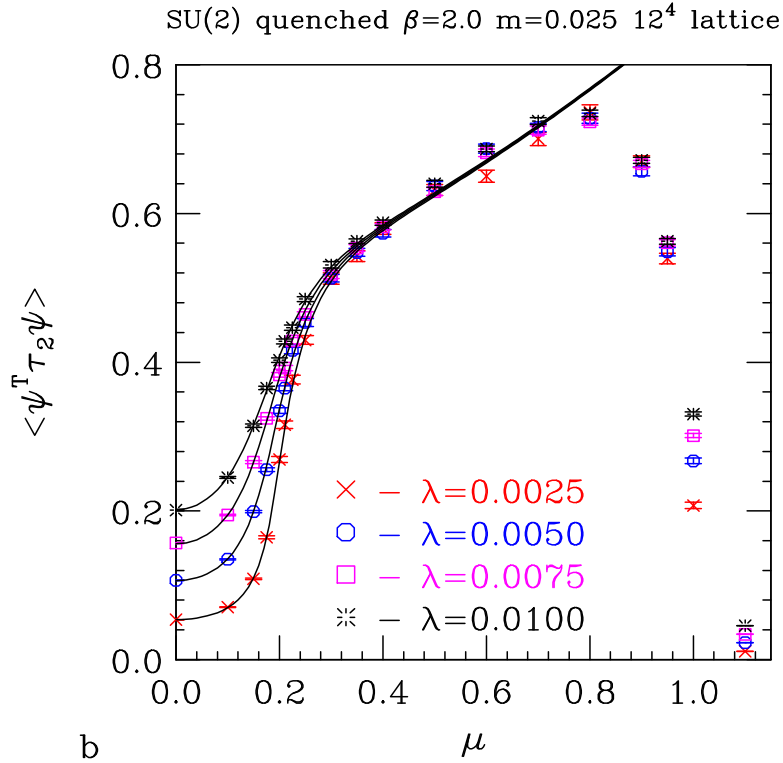
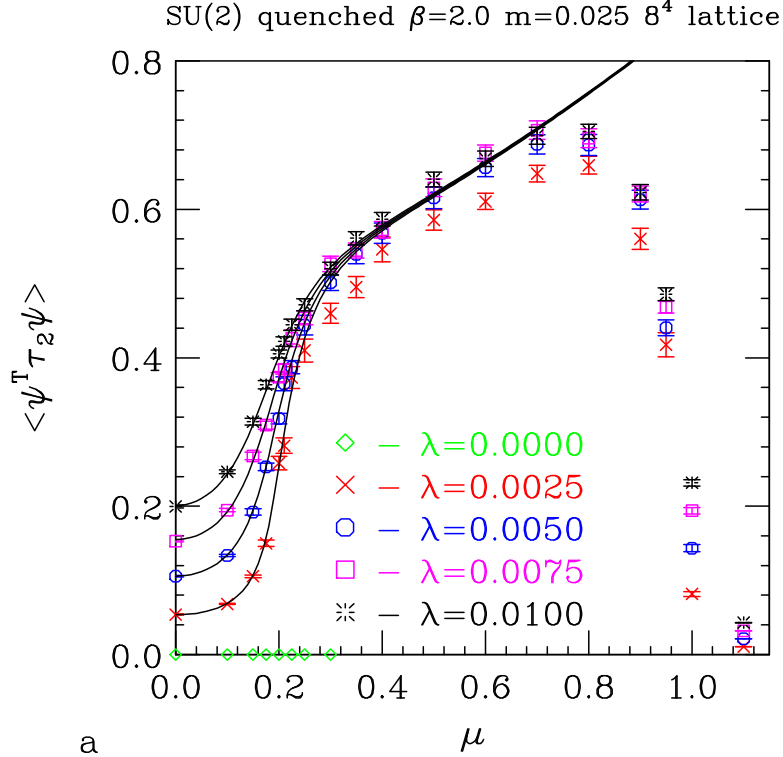


FIG. 7: The diquark condensate for quenched 2-colour QCD as a function of μ and λ on at $\beta = 2.0$ a) on an 8^4 lattice and b) on a 12^4 lattice. The curves are the scaling fits described in section 4.

this condensate increases monotonically with μ up to $\mu \sim 0.7$ after which it falls due to

saturation effects. Qualitatively this curve is very similar to the corresponding curve with dynamical quarks. It is also very similar to the curve for QCD at finite isospin chemical potential at $\beta = 5.5$ especially when one observes that we should equate μ_I with 2μ . As in that case, the condensate increases relatively rapidly as μ is increased beyond μ_c . (This will be made quantitative in the next section.) We note that the $\lambda = 0.0025$ measurements on the 8^4 lattice show signs of finite size effects for larger μ values, which is why we repeated these simulations on a 12^4 lattice where these effects have been considerably reduced.

SU(2) quenched $\beta=2.0$ $m=0.025$ 12^4 lattice

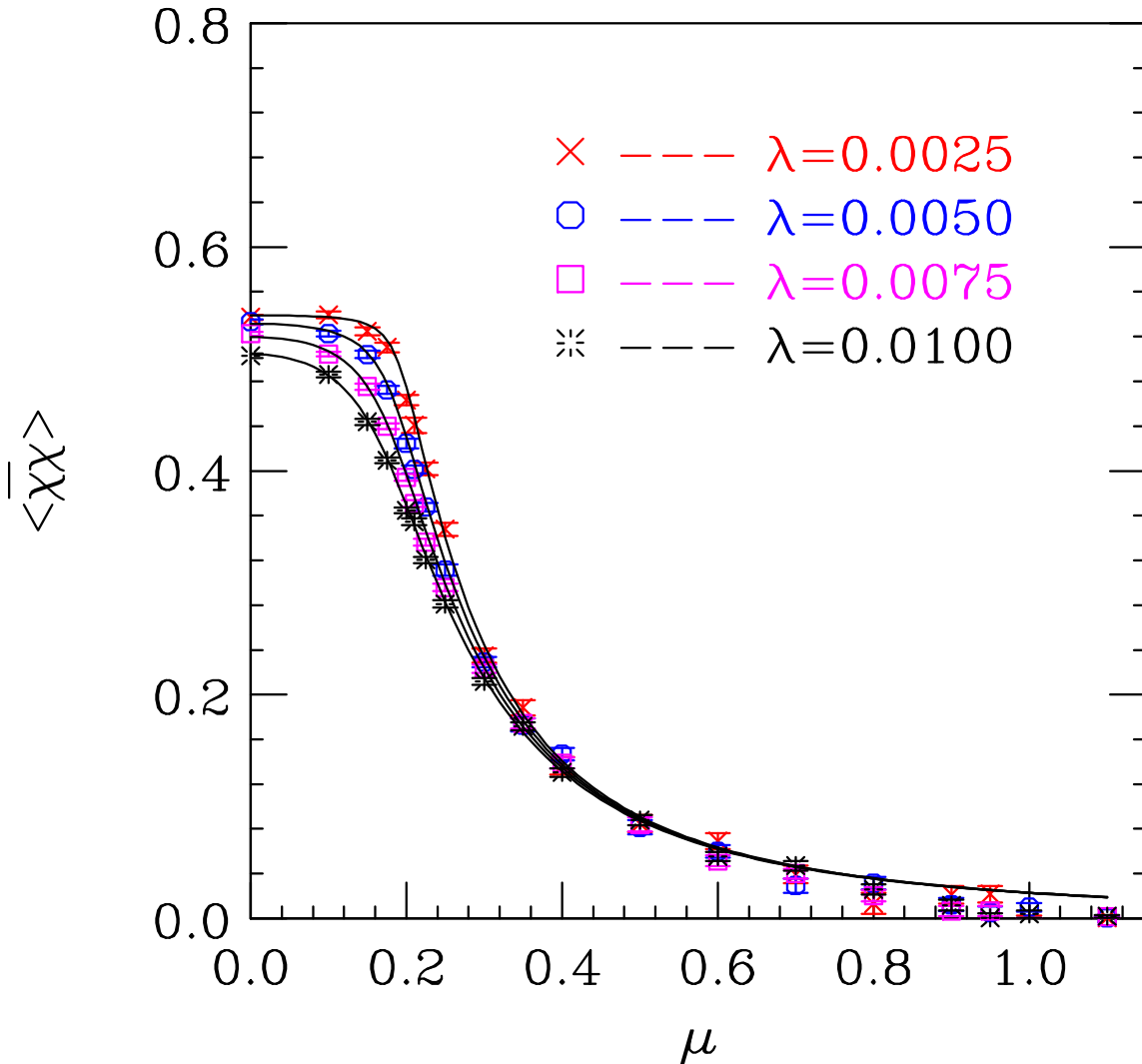


FIG. 8: Chiral condensate as a function of μ and λ , for 2-colour QCD at finite chemical potential for quark number on a 12^4 lattice. The solid lines are the fits given in the next section.

In figure 8 we show the chiral condensates as functions of μ for the 4 λ values given

above (and $\lambda = 0$ for $\mu \leq 0.2$). (We present only the 12^4 ‘data’ since there is little difference between the 2 lattice sizes.) For $\mu < \mu_c$ this graph is consistent with the expectation that the $\lambda \rightarrow 0$ limit should be μ independent. As μ is increased beyond μ_c , the condensate falls. This agrees with the expectation that the condensate is rotating from the chiral to the diquark direction in this region. One notes, however, that this is not a simple rotation since the magnitude of the condensate also increases with μ for larger μ values until saturation effects appear. The general appearance of this curve is similar to those with dynamical quarks and to those for QCD at finite isospin density.

SU(2) quenched $\beta=2.0$ $m=0.025$ 12^4 lattice

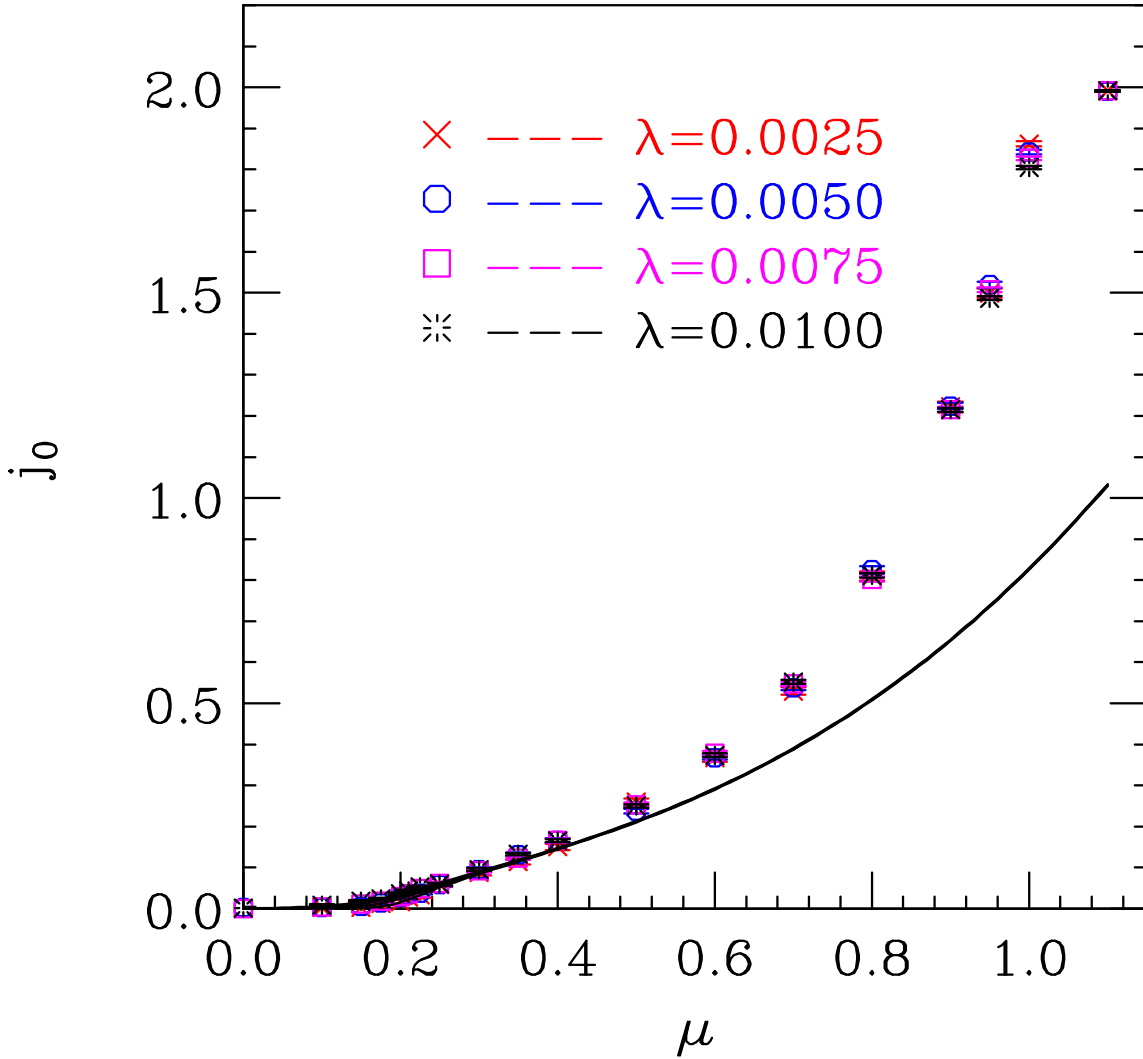


FIG. 9: Quark-number density j_0 as a function of μ and λ on

The quark-number density is shown in figure 9 as a function of μ for each of the considered λ values mentioned above. (Again, because the finite size effects are small, we present only the 12^4 ‘data’). We see that j_0 is consistent with zero for small μ , and rises slowly from zero above μ_c . The rise becomes more rapid for $\mu \gtrsim 0.6$. The density finally saturates at 2 — 2 colours of staggered fermions per site — due to fermi statistics, a finite lattice spacing effect. Note that there is little if any λ dependence. This behaviour is very similar to that of j_0^3 for our quenched QCD at finite μ_I , except that there the saturation value is 3 rather than 2 since this number merely counts colours. Again we note the similarity of these quenched results to those obtained with dynamical quarks.

The qualitative behaviour of all the ‘data’ presented in this section is in agreement with what is predicted from effective Lagrangians using the methods of chiral perturbation theory. We have noted that the condensate does not simply rotate from the chiral direction into the quark-number or isospin violating direction which was the prediction of tree level chiral perturbation theory [1, 10], but rather rotates and increases in magnitude. Such behaviour is seen when the chiral perturbation theory includes next-to-leading order terms including 1-loop contributions [11]. Of course, the one effect that effective Lagrangians cannot see is saturation, since they do not describe the underlying fermions of the theory. However, as we have pointed out, saturation is a finite lattice spacing effect, and is thus of limited interest.

IV. CRITICAL SCALING AND THE EQUATION OF STATE.

Analyses of effective Lagrangians using the methods of chiral perturbation theory give predictions for the critical exponents and the scaling of the order parameter(s) close to the critical point μ_c , both for 2-colour QCD at finite μ and for QCD at finite μ_I . Clearly the tree level analyses will give mean-field scaling with critical exponents $\beta_m = \frac{1}{2}$ and $\delta = 3$ [1, 10]. More recent analyses have extended these results to next-to-leading order including 1-loop corrections for 2-colour QCD, and find that the critical indices remain at their mean-field values [11]. However, the tree-level result that the magnitude of the total condensate is independent of μ and λ no longer holds. One can thus speculate that scaling with mean-field exponents holds to all orders. The effective Lagrangian for QCD at finite μ_I is so similar

as to lead to the expectation that this theory also has mean field behaviour through next-to-leading order and perhaps to all orders. Simulations of 2-colour QCD at finite μ in the strong coupling limit [8] also indicate mean-field scaling with a scaling function consistent with that of lowest order tree-level effective Lagrangian predictions.

The two critical exponents relevant to the scaling of the charged pion condensate — the order parameter for the transition we are considering — are β_m and δ defined as follows. At $m = 0$,

$$i\langle\bar{\psi}\gamma_5\tau_2\psi\rangle \rightarrow \text{const}(\mu_I - \mu_c)^{\beta_m} \quad (12)$$

as $\mu_I \rightarrow \mu_c+$ (and vanishes for $\mu_I \leq \mu_c$). For $\mu_I = \mu_c$,

$$i\langle\bar{\psi}\gamma_5\tau_2\psi\rangle \rightarrow \text{const } m^{\frac{1}{\delta}} \quad (13)$$

as $m \rightarrow 0+$. The mean-field values of these 2 exponents are $\beta_m = \frac{1}{2}$ and $\delta = 3$. Analogous definitions hold for 2-colour QCD.

We shall be considering 3 different forms for the scaling function, i.e. for the equation of state, each of which exhibits mean-field scaling. Indeed, sufficiently close to the critical point they give identical scaling functions for the order parameter. Our later discussions will make it clear why, in practical applications, it is important to have a more detailed knowledge of the scaling function.

The first form for the equation of state is that suggested by the lowest order tree-level analysis of the effective Lagrangians of [1, 10], which are of the non-linear sigma model form. It derives from the value of the parameter α which minimizes the effective potential

$$\mathcal{E} = -a \mu^2 \sin^2(\alpha) - b m \cos(\alpha) - b \lambda \sin(\alpha) \quad (14)$$

in terms of which

$$\langle\chi^T\tau_2\chi\rangle = b \sin(\alpha) \quad (15)$$

$$\langle\bar{\chi}\chi\rangle = b \cos(\alpha) \quad (16)$$

and

$$j_0 = 2 a \mu \sin^2(\alpha). \quad (17)$$

b is given in terms of μ_c and a , namely

$$b = \frac{2}{m} a \mu_c^2 \quad (18)$$

and the scaling forms of the observables for $\lambda = 0$, expressed in terms of the scaling variable $x = \mu/\mu_c$, are

$$\langle \chi^T \tau_2 \chi \rangle = b \sqrt{1 - \frac{1}{x^4}} \quad (19)$$

$$\langle \bar{\chi} \chi \rangle = b \frac{1}{x^2} \quad (20)$$

and

$$j_0 = 2 a \mu \left(1 - \frac{1}{x^4}\right) \quad (21)$$

Note that the equivalent form for QCD at finite μ_I has an extra factor of 2 in the equation for j_0^3 because of our normalization. Otherwise the forms are identical with μ replaced with μ_I . The main deficiency with this form is that it requires that the magnitude of the condensate, $\sqrt{\langle \chi^T \tau_2 \chi \rangle^2 + \langle \bar{\chi} \chi \rangle^2}$ to be constant independent of μ and λ . This is not even true in next-to-leading order chiral perturbation theory [11] and has at best a limited range of validity in our simulations.

To allow the norm of the condensate to increase with μ and possibly λ , we consider a second form for the equation of state which is derived from an effective Lagrangian of the linear sigma model type. This is obtained by extracting the values of R and α which minimize the effective potential

$$\mathcal{E} = \frac{1}{4} R^4 - \frac{1}{2} a R^2 - \frac{1}{2} b \mu^2 \sin^2(\alpha) - c m R \cos(\alpha) - c \lambda R \sin(\alpha) \quad (22)$$

in terms of which

$$\langle \chi^T \tau_2 \chi \rangle = c R \sin(\alpha) \quad (23)$$

$$\langle \bar{\chi} \chi \rangle = c R \cos(\alpha) \quad (24)$$

and

$$j_0 = b \mu R^2 \sin^2(\alpha). \quad (25)$$

c is given in terms of μ_c by

$$c = \frac{b \mu_c^2}{m} \sqrt{a + b \mu_c^2} \quad (26)$$

When $\lambda = 0$ we obtain the scaling forms

$$\langle \chi^T \tau_2 \chi \rangle = c \sqrt{a + b \mu_c^2 x^2 - (a + b \mu_c^2) \frac{1}{x^4}} \quad (27)$$

$$\langle \bar{\chi} \chi \rangle = c \sqrt{a + b \mu_c^2} \frac{1}{x^2} \quad (28)$$

and

$$j_0 = b \mu \left[a + b \mu_c^2 x^2 - (a + b \mu_c^2) \frac{1}{x^4} \right]. \quad (29)$$

Again j_0^3 has an extra factor of 2 for QCD at finite μ_I .

Finally we consider the simplest mean-field equation of state [22] which considers only the scaling of the order parameter (diquark or charged pion condensate) near the transition and does not even attempt to address chiral symmetry breaking. This is given in terms of ϕ which minimizes the effective potential

$$\mathcal{E} = \frac{1}{4}\phi^4 - \frac{1}{2}a(\mu - \mu_c)\phi^2 - b\lambda\phi. \quad (30)$$

In terms of ϕ ,

$$\langle \chi^T \tau_2 \chi \rangle = b \phi \quad (31)$$

and

$$j_0 = a \phi^2. \quad (32)$$

Once again j_0^3 has an extra factor of 2 for QCD at finite μ_I . When $\lambda = 0$ we find the simple scaling relations for $\mu > \mu_c$

$$\langle \chi^T \tau_2 \chi \rangle = b \sqrt{a(\mu - \mu_c)} \quad (33)$$

and

$$j_0 = a^2(\mu - \mu_c). \quad (34)$$

We start by considering quenched QCD at finite μ_I at $\beta = 5.5$. We first fit our measurements of the pion condensate to the form suggested by the non-linear sigma-model effective Lagrangian (equations 14,15). The quark mass is treated as a fitting parameter. Here we find a good fit over the range $0 \leq \mu_I \leq 0.7$, and all 3 λ values with $\mu_c = 0.422(2)$, $a = 0.0618(8)$ and $m = 0.0267(2)$ with a confidence level of 61%. The range limitation is due to the fact that the norm of the condensate is only approximately constant over a limited range of μ_I . The departure of the mass m from its input value is presumably also a reflection of this. We then fit our pion condensate ‘data’ to the form suggested by the linear sigma-model effective Lagrangian (equations 22,23). With this form, our fits constrain the mass parameter, m , to be so close to the input mass that we choose to set $m = 0.025$ in our fits. We then obtain an excellent fit over to the pion condensate over the range $0 \leq \mu_I \leq 1.4$ with $\mu_c = 0.419(2)$, $a = 0.412(7)$, $b = 0.242(4)$ and a confidence level of 92%. We have

superimposed these fits on the graphs of our ‘data’ in figure 4. These fits give predictions for the chiral condensate and isospin density (equations 24,25) which we have included in the plots of our measurements of these quantities in figures 5,6. The predicted chiral condensate is clearly in good agreement with our measurements. The predicted isospin density is in good agreement with measurements up to $\mu_I \approx 1.0$. Note that the isospin density has been predicted to be proportional to μ_I^3 at large μ_I [1] so that the predictions of equation 25 are guaranteed to break down, even if we did not have the effects of saturation.

Let us now turn our attention to our simulations of 2-colour QCD at finite μ . First let us consider fits to our 8^4 measurements. Here we again note that our fits to the non-linear sigma model scaling form can only be made over a somewhat limited domain of μ . This can be extended by using the linear sigma model scaling forms, but only when we neglect the $\lambda = 0.0025$ measurements which show clear signs of finite size effects at large μ . Fitting the $\lambda = 0.005, 0.0075, 0.01$ ‘data’ we obtained a fit over the range $0 \leq \mu \leq 0.7$ with $\mu_c = 0.209(1)$, $a = 0.405(9)$, $b = 0.71(2)$ and a 77% confidence level. To reduce the finite size errors, especially at $\lambda = 0.0025$, we repeated these simulations on a 12^4 lattice. Here our best fit, obtained using all 4 λ values and fitting over the range $0 \leq \mu \leq 0.4$, gave $\mu_c = 0.2066(4)$, $a = 0.405(9)$ and $b = 0.73(1)$ at a confidence level of 10% ($\chi^2/dof = 1.3$). Although we have reduced our finite size effects by going to a larger lattice, we have also reduced the statistical errors, making the remaining finite size effects more important. We suspect that this is at least part of the reason that we have obtained a worse fit on the larger lattice. These fits for the pion condensate are shown in figure 7. The predictions for the chiral condensate and quark-number density which these fits provide are superimposed on the plots of measured values for the 12^4 lattice in figures 8,9. It is clear that the prediction for the chiral condensate provides good fits to the ‘data’. The predicted quark-number density is also a good fit to the ‘data’ for $\mu_I \leq 0.4$.

Finally we turn to the consideration of the $\beta = 5.7$ quenched QCD simulations at finite μ_I . After producing ‘data’ over the range $0 \leq \mu_I \leq 2.1$ for $\lambda = 0.0025, 0.005, 0.0075$ on a $12^3 \times 24$ lattice, we performed simulations on a 16^4 lattice over the range $0.2 \leq \mu_I \leq 0.7$ at $\lambda = 0.000625, 0.00125, 0.001875, 0.0025$ to probe the transition more closely. Not surprisingly, considering that the norm of the condensate grows rapidly in the broken symmetry phase, fits to the non-linear sigma model scaling proved fruitless. We fit our

16^4 measurements the linear sigma model equation of state, treating the quark mass as a fitting parameter. We exclude the $\lambda = 0.000625$ measurements from our fits since they show clear finite size effects at larger μ_I . Our ‘best’ fit to the $\lambda = 0.00125, 0.001875, 0.0025$ measurements gives $\mu_c = 0.4500(7)$, $a = 7.00(1)$, $b = 0.266(7)$, $m = 0.0212(4)$ with $\chi^2/dof = 1.7$ and a confidence level of only 0.3%. This indicates that while the linear sigma model equation of state remains a good guide to the critical behaviour quenched QCD at finite μ_I at $\beta = 5.7$, the data is beginning to show small, but non-negligible departures from this simple form. We have superimposed these fits on the ‘data’ of figure 1 to indicate that they are a good qualitative fit to the data. We note also that the predicted μ_c is close to the measured pion mass $m_\pi = 0.441(1)$. Because $m \neq 0.025$ in these fits, we do not expect the predictions for the chiral condensate to be good. In fact, what we see is that the fits are suppressed relative to the data roughly in the ratio of the fitted mass to the input mass (0.025). Next we plot the values of j_0^3 predicted using equation 25 to compare with measurements in figure 3. We see that there is good agreement out to $\mu_I = 1.0$. Finally, we fit the pion condensate at $\mu_I = 0.45$ which is very close to μ_c to the scaling form of equation 13. For this we use the measured values on the 16^4 lattice at $\lambda = 0.000625, 0.00125, 0.001875, 0.0025$ and those from the $12^3 \times 24$ lattice at $\lambda = 0.005, 0.0075$. From this we obtain $\delta = 3.25(7)$ with a confidence level of 27%. Dropping the 2 largest λ values gives $\delta = 2.88(16)$ with an 85% confidence level. These fits are in good agreement with the mean field value $\delta = 3$.

The effective Lagrangian approach seeks to give a uniform description of both chiral symmetry breaking and isospin (or quark-number) breaking. Thus we should only expect physics to be insensitive to the details of the effective Lagrangian/effective potential when the quark mass is small enough that the order m or equivalently order m_π^2 corrections are small. One measure of this is how much the chiral condensate $\langle \bar{\psi}\psi \rangle$ at the quark mass we use differs from its zero mass value. At $\beta = 5.5$, $\langle \bar{\psi}\psi \rangle(m = 0.0125) = 0.729(11)$, $\langle \bar{\psi}\psi \rangle(m = 0.025) = 0.764(7)$ and $\langle \bar{\psi}\psi \rangle(m = 0.05) = 0.838(5)$, so the difference is $\sim 10\%$ which should be small enough. At $\beta = 5.7$, $\langle \bar{\psi}\psi \rangle(m = 0.00625) = 0.288(3)$, $\langle \bar{\psi}\psi \rangle(m = 0.0125) = 0.323(2)$, $\langle \bar{\psi}\psi \rangle(m = 0.025) = 0.386(2)$ and $\langle \bar{\psi}\psi \rangle(m = 0.05) = 0.494(2)$, so the difference is $\sim 50\%$ and the detailed form of the effective potential might be expected to be important. We believe that this is for this reason why the simple ansatz for the effective potential/equation of state works so well at $\beta = 5.5$ but shows limitations at $\beta = 5.7$.

We end this section with a discussion of the behaviour of different variables which describe the scaling in terms of $\mu(\mu_I)$. For convenience we express them in terms of $x = \mu/\mu_c(\mu_I/\mu_c)$. The simplest is $x - 1$ which is the scaling variable of the simplest mean-field equation of state. The next, $\frac{1}{4}(1 - 1/x^4)$, is that of the non-linear sigma model (or the linear sigma model in the limit $a \rightarrow \infty$). The third, $\frac{1}{6}(x^2 - 1/x^4)$ is that for the linear sigma model in the limit as $a \rightarrow 0$. This third form gives a reasonable description of the scaling of $\beta = 5.7$ ‘data’ on the $12^3 \times 24$ lattice, in the ordered ($\mu_I \geq \mu_c$) phase. All 3 scaling variables behave identically as $x \rightarrow 1$, however, a poor choice leads to a severely curtailed scaling window. $x - 1$ and $\frac{1}{4}(1 - 1/x^4)$ already differ by $\sim 10\%$ at $x = 1.04$. $x - 1$ and $\frac{1}{6}(x^2 - 1/x^4)$ differ by $\sim 10\%$ at $x = 1.08$. Thus, for practical reasons, we should make a wise choice of scaling variables.

However, we have noted apparent mean-field scaling of our $\beta = 5.7$ pion condensate in the ordered phase both in terms of the simplest mean-field scaling forms where the scaling variable is $x - 1$, and in terms of the linear sigma model form where the scaling variable is approximately $\frac{1}{6}(x^2 - 1/x^4)$, out to $x \sim 1.8$. Only by examining the scaling very close to the transition and including $\mu_I < \mu_c$ measurements in the fit, were we able to determine that the linear sigma model form gave the better description of the transition. The reason for this is that $\frac{1}{6}(x^2 - 1/x^4)$ has a point of inflection at $x = \sqrt[6]{10} = 1.467\dots$, at which it is again linear in x . In the neighbourhood of this point of inflection $\frac{1}{6}(x^2 - 1/x^4) \propto x - x_0$, where $x_0 = (5/8)\sqrt[6]{10} = 0.917\dots$, so this defines another *larger* region where $\frac{1}{6}(x^2 - 1/x^4)$ is linear in x , and the linear approximation has an intercept not too far from the true critical point. It is this linearity, which gives us an (apparent) extended scaling regime. Over the region where the scaling variable is approximately linear in x , we will observe scaling with the correct exponent, β_m . Of course, the coefficient of this apparent scaling form will differ from the correct coefficient.

It is instructive to also look at the properties of $\frac{1}{4}(1 - 1/x^4)$ as a function of x . It clearly does not have a point of inflection, however, its square has a point of inflection at $x = \sqrt[4]{9/5} = 1.158\dots$ about which it too becomes linear. This linear approximation has its intercept at $x_0 = (9/10)\sqrt[4]{9/5} = 1.042\dots$, which is again near to the critical point. Since it is the square of the scaling variable that has this point of inflection, this leads to apparent scaling with a critical exponent, β_m of half the true value. In the case of a mean-field critical

point this pseudo-exponent will be $\frac{1}{4}$, which is β_m for a tricritical point. If we restrict ourselves to the ordered phase, it is possible to fit the order parameter for QCD at finite μ_I at $\beta = 5.5$ and that for 2-colour QCD at finite μ at $\beta = 2.0$ to a tricritical scaling form — equation 30 with $\frac{1}{4}\phi^4$ replaced by $\frac{1}{6}\phi^6$. Hence one should be suspicious if an order parameter scales with a critical exponent which is half of what one expects.

V. DISCUSSION AND CONCLUSIONS

Gauge theories with fermions at finite chemical potential for a conserved charge, which have positive fermion determinants, have sensible quenched approximations. This contrasts with QCD at a finite chemical potential for baryon/quark number, where the quenched limit is really the quenched limit for QCD with equal numbers of quarks with quark-number ± 1 and not that for QCD with all quarks having quark-number $+1$.

We have studied the quenched versions of QCD at finite chemical potential (μ_I) for isospin, and of 2-colour QCD at finite chemical potential (μ) for quark number. We included an explicit symmetry breaking term with strength λ in each case. What we find is that for $\lambda \rightarrow 0$ this symmetry — I_3 for QCD at finite μ_I , quark-number for 2-colour QCD — is unbroken for small $\mu(\mu_I)$. In each case there is a critical value for μ_I or μ (μ_c say), above which a condensate forms which breaks the relevant symmetry spontaneously. In our QCD at finite μ_I measurements at $\beta = 5.7$ on a $12^3 \times 24$ lattice, we also measured the pion mass at $\mu_I = \lambda = 0$, and found it to be close to our estimates for μ_c as expected. In QCD at finite μ_I this is a charged pion condensate while for 2-colour QCD it is a diquark condensate. This is precisely the behaviour expected and seen for the full (unquenched) theories. The transition appears to be second order as was observed and expected in the full theories. For high $\mu_I(\mu)$ saturation effects due to fermi statistics drive the condensates to zero which is also observed for the full theories and is a finite lattice spacing effect. Thus these quenched theories are useful to study since they require far less computing time than the full theories — these studies were performed on 400MHz PC's supplemented with a few days running on an IBM SP whereas the full theories require many months of IBM SP running.

We studied the scaling of the order parameter, $i\langle\bar{\psi}\gamma_5\tau_2\psi\rangle$ (the charged pion condensate), for QCD at finite μ_I , and $\langle\chi^T\tau_2\chi\rangle$ (the diquark condensate) for 2-colour QCD at

finite μ and saw evidence that the mean field equation of state was the correct one in the neighbourhood of the critical point. This required using scaling forms implied by effective Lagrangian analyses, in order to use scaling variables which maximize the scaling window and make scaling analyses practical. Because of this sensitivity to the choice of scaling variables, these conclusions cannot be considered conclusive. In the quenched theory, it might be feasible to extend these simulations to much larger lattices and much smaller λ values, enabling one to probe sufficiently close to the critical point to be insensitive to the choice of scaling variables. However, here one runs the risk of being frustrated by the pathologies of quenching. For the dynamical theories the expense (in computing resources) of simulating on large lattices with very small λ values is prohibitive. We have noted that even by couplings as small as that at $\beta = 5.7$, the simple scaling forms suggested by effective Lagrangian analyses are barely adequate at the quark mass we use ($m = 0.025$ in lattice units), and a better choice is desirable and probably essential at weaker couplings. While it is easy enough to produce variant forms of the effective potential and the equations of state they imply, one needs a form which improves the fits, without introducing too many extra parameters and preferably one motivated by physics or chiral perturbation theory.

On examining the detailed properties of proposed scaling variables, we have found that a certain class has a point of inflection, when expressed in terms of the simplest scaling variable. This leads to an extended region of apparent scaling which is a precursor of true scaling. In dynamical theories where one cannot probe the true scaling window, this might be the best indicator we have of the nature of critical scaling. However, as we have noted, certain other proposed scaling variables which lack such a point of inflection, have squares which *do* have such a point of inflection, leading to apparent scaling with a critical index β_m which is half of the true value, potentially leading one to erroneous conclusions.

Once the fit to the pion or diquark condensate provides the parameters for the appropriate effective potential, this provides a prediction for the isospin or quark-number density. These predictions are in good agreement with our direct measurements of these ‘charge’ densities within the scaling window. In addition, the effective potential provides a prediction of the chiral condensate. For quenched QCD at finite μ_I at $\beta = 5.5$ and quenched 2-colour QCD at finite μ at $\beta = 2.0$, where the fits require a quark mass m in good agreement with the input value ($m = 0.025$), the predicted chiral condensates are in good agreement with

the measured values. In quenched QCD at finite μ_I at $\beta = 5.7$, where the fits require m to be appreciably lower than the input value, the predictions for the corresponding chiral condensate are similarly lower. This we tentatively attribute to the fact that the higher order terms in a chiral expansion (expansion in powers of m) are large at $\beta = 5.7$, $m = 0.025$. Where the predictions from our proposed equation of state are in good agreement with measurements, they support our claim that there is a critical point at $\mu(\mu_I) = \mu_c$, $\lambda = 0$, with mean field exponents.

We have just completed further simulations of 2-colour QCD at finite quark-number chemical potential with dynamical quarks which examine the critical scaling at the transition from the normal phase to the diquark-condensed phase in which we also see evidence for mean-field scaling [26]. In addition, we are performing simulations of QCD at finite chemical potential for isospin(I_3) [2, 3] and see evidence for mean field scaling [3].

We are extending the work of this paper to include a strange quark with its own chemical potential. This work will study the competition between charged pion and kaon condensation as the 2 chemical potentials are varied independently. Chiral perturbation theory predicts that the phases with pion and kaon condensates are separated by a first order phase transition. Here the quenched approximation will make it easy to study the phase structure of the plane defined by the 2 chemical potentials.

Acknowledgements

DKS was supported by DOE contract W-31-109-ENG-38. JBK was supported in part by an NSF grant NSF PHY-0102409. IBM SP access was provided at NERSC. DKS would like to thank the Special Research Centre for the Subatomic Structure of Matter of the University of Adelaide where this work was completed. He would also like to thank C. K. Zachos and G. T. Bodwin for helpful discussions. JBK wishes to thank D. Toublan for many useful discussions.

[1] D. T. Son and M. A. Stephanov, Phys. Rev. Lett. 86, 592 (2001); D. T. Son and M. A. Stephanov, Phys. Atom. Nucl. 64, 834 (2001), Yad. Fiz. 64, 899 (2001).

- [2] J. B. Kogut and D. K. Sinclair, Nucl. Phys.(Proc. Suppl.) 106, 444, (2002).
- [3] J. B. Kogut and D. K. Sinclair, e-print hep-lat/0202028 (2002).
- [4] S. E. Morrison and S. J. Hands, in "Strong and Electroweak Matter '98'," edited by J. Ambjørn et al., p. 364.
- [5] S. Hands, J. B. Kogut, M.-P. Lombardo, and S. E. Morrison, Nucl. Phys. B558, 327 (1999).
- [6] J. B. Kogut, D. Toublan, and D. K. Sinclair, Phys. Lett. B514, 77 (2001)
- [7] J. B. Kogut, D. K. Sinclair, S. J. Hands, S. E. Morrison, Phys. Rev. D64, 094505 (2001).
- [8] R. Aloisio, V. Azcoiti, G. Di Carlo, A. Galante, and A. F. Grillo, Phys. Lett. B 493, 189 (2000); R. Aloisio, V. Azcoiti, G. Di Carlo, A. Galante, and A. F. Grillo, Nucl. Phys. B606, 322 (2001).
- [9] S. Muroya, A. Nakamura, C. Nonaka, e-print nucl-th/0111082 (2001).
- [10] J. B. Kogut, M. A. Stephanov and D. Toublan, Phys. Lett. B464, 183 (1999). J. B. Kogut, M. A. Stephanov, D. Toublan, J. J. M. Verbaarschot and A. Zhitnitsky, Nucl. Phys. B582, 477 (2000).
- [11] K. Splittorff, D. Toublan and J. J. M. Verbaarschot, e-print hep-ph/0108040 (2001).
- [12] B. C. Barrois, Nucl. Phys. B129, 390 (1977)
- [13] D. Bailin and A. Love, Phys. Rept. 107, 325 (1984).
- [14] M. Alford, K. Rajagopal and F. Wilczek, Phys. Lett. B222, 247 (1998); M. Alford, K. Rajagopal and F. Wilczek, Nucl. Phys. B537, 443 (1999); T. Schäfer and F. Wilczek, Phys. Rev. D60, 074014 (1999); T. Schäfer and F. Wilczek, Phys. Rev. D60, 114033 (1999).
- [15] R. Rapp, T. Schafer, E. V. Shuryak and M. Velkovsky, Phys. Rev. Lett. 81, 53 (1998)
- [16] Good recent reviews include: M. Alford, Nucl. Phys. B(Proc. Suppl.) 73, 161 (1999); E. Shuryak, Nucl. Phys. B(Proc. Suppl.) 83-84, 103 (2000); K. Rajagopal and F. Wilczek, e-print hep-ph/0011333 (2000).
- [17] I. Barbour, Nucl. Phys. B(Proc. Suppl.)26, 22 (1992).
- [18] I. Barbour, N. E. Behilil, E. Dagotto, F. Karsch, A. Moreo, M. Stone, and H. W. Wyld, Nucl. Phys. B 275 [FS17], 296 (1986).
- [19] C. T. H. Davies and E. G. Klepfish, Phys. Lett. B 256, 68 (1991), and references contained therein.
- [20] M.A. Stephanov, Phys. Rev. Lett. 76, 4472 (1996).
- [21] J. B. Kogut, M.-P. Lombardo and D. K. Sinclair, Phys. Rev. D51, 1282 (1995); Phys. Rev.

- D54, 2303 (1996).
- [22] See for example: C. Itzykson and J-M Drouffe, “Statistical Field Theory”, Vol. 1, Chapter 3, Cambridge University Press (1989).
- [23] S. R. Sharpe, Phys. Rev. D41, 3233 (1990); S. R. Sharpe, Phys. Rev. D46, 3146 (1992); C. Bernard and M. Golterman, Nucl. Phys. B(Proc. Suppl.)26, 360 (1992); C. W. Bernard and M. F. L. Golterman Phys. Rev. D46, 853 (1992).
- [24] J. B. Kogut and D. K. Sinclair, Phys. Lett. B492, 228 (2000); J. B. Kogut and D. K. Sinclair, Phys. Rev. D64, 034508 (2001).
- [25] I. D. Lawrie and S. Sarbach, in *Phase Transitions and Critical Phenomena, Volume 9* (Academic Press, London, 1984).
- [26] J. B. Kogut, D. Toublan, and D. K. Sinclair (in preparation).